World Academy of Science, Engineering and Technology
International Journal of Aerospace and Mechanical Engineering
Vol:3, No:9, 2009

Siding Mode Control of Pitch-Rate of an F-16 Aircraft

Ekprasit Promtun* and Sridhar Seshagiri, *Member, IEEE*

***Abstract*—** This paper considers the control of the longitudinal flight dynamics of an F-16 aircraft. The primary design objective is model-following of the pitch rate q, which is the preferred system for aircraft approach and landing. Regulation of the aircraft velocity V (or the Mach-hold autopilot) is also considered, but as a secondary objective. The problem is challenging because the system is nonlinear, and also non-affine in the input. A sliding mode controller is designed for the pitch rate, that exploits the modal decomposition of the linearized dynamics into its short-period and phugoid approximations. The inherent robustness of the SMC design provides a convenient way to design controllers without gain scheduling, with a steady-state response that is comparable to that of a conventional polynomial based gain-scheduled approach with integral control, but with improved transient performance. Integral action is introduced in the sliding mode design using the recently developed technique of "conditional integrators", and it is shown that robust regulation is achieved with asymptotically constant exogenous signals, without degrading the transient response. Through extensive simulation on the nonlinear multiple-input multiple-output (MIMO) longitudinal model of the F-16 aircraft, it is shown that the conditional integrator design outperforms the one based on the conventional linear control, without requiring any scheduling.

***Keywords*—** Sliding-mode Control, Integral Control, Model Following, F-16 Longitudinal Dynamics, Pitch-Rate Control.

I. Introduction

THE dynamic response characteristics of aircraft are highly nonlinear. Traditionally, flight control systems have been designed using mathematical models of the aircraft linearized at various flight conditions, with the controller parameters or gains "scheduled" or varied with the flight operating conditions. Various robust multivariable techniques including linear quadratic optimal control (LQR/LQG), H_∞ control, and structured singular value μ-synthesis have been employed in controller design, an excellent and exhaustive compendium of which is available in [15]. In order to guarantee stability and performance of the resulting gain-scheduled controllers, analytical frameworks of gain scheduling have been developed (see, for example, [11]), including the powerful technique of linear-parameter-varying (LPV) control (see, for example, [4], [5], [13], [14], [24], [28]). Nonlinear design techniques such as dynamic inversion have been used in [1], [19], [26], while a technique that combines model inversion control with an online adaptive neural network to "robustify" the design is described in [21], and a nonlinear adaptive design based on backstepping and neural networks in [12]. A succinct "industry perspective" on flight control design, including the techniques of robust control (H_∞, μ-synthesis), LPV control, dynamic inversion, adaptive control, neural networks, and more, can be found in [2].

Our interest is in the design of robust sliding mode control (SMC) for the longitudinal flight dynamics of a F-16 aircraft that is not based on LPV models or gain-scheduling. LPV/gain-scheduling based designs for a F-16 have been pursued, for example, in [7], [9], [13], [14]. The application of SMC to flight control has been pursued by several others authors, for example, [6], [8], [25]. Our work differs from earlier ones in that it is based on a recent technique in [22] for introducing integral action in SMC. While we design a nonlinear controller, it is designed based upon plant linearization. In particular, our design exploits the modal decomposition of the linearized dynamics into its short-period and phugoid approximations. Our primary emphasis is on the transient and steady-state performance of control of the aircraft's pitch rate, with the steady-state performance and disturbance rejection of the aircraft's velocity as a (minor) secondary objective. The desired transient and steady-state specifications for the pitch rate are encapsulated in the response of a reference model, and the (SMC) controller is designed as a model-following controller. As a consequence of exploiting the modal decomposition of the aircraft dynamics, the pitch rate controller has a very simple structure. It is simply a high-gain PI controller with an "anti-windup" integrator, followed by saturation. This controller structure is a special case of a general design for robust output regulation for multiple-input multiple-output (MIMO) nonlinear systems transformable to the normal form, with analytical results for stability and performance described in [22]. Through extensive simulations, we show that this design outperforms a traditional gain-scheduled controller design based on the polynomial approach to model-following design. A preliminary version of this paper appeared in the Proceedings of the 17th IFAC World Congress in Seoul, 2008 [18].

The rest of this paper is organized as follows. In Section 2, we describe the nonlinear mathematical aircraft model, its linearization and the decomposition of the dynamics into the short-period and phugoid modes. This section is extracted mostly from [29], with the Simulink model for simulation purposes based on [20]. The design of the pitch controller based on the "conditional integrator" SMC design of [22] is taken up in Section 3, and simulation results showing the efficacy of the design, along with comparisons to gain scheduled controllers using the (linear) transfer-function based polynomial approach to model-following are presented in Sec-

E. Promtun is with the Aircraft Research and Development Office, The Royal Thai Air Force, Bangkok, Thailand e-mail: promtun@rohan.sdsu.edu.
S. Seshagiri is with the ECE Dept., San Diego State University, San Diego, CA 92182, USA e-mail: seshagir@engineering.sdsu.edu.
*Financially supported in part by the Royal Thai Air Force.

tion 4. Finally, a summary of our work and some suggestions for possible extensions are provided in Section 5.

II. 3-DOF Longitudinal Model

The equations for pure longitudinal motion of an aircraft with no thrust-vectoring can be described by the 5th order nonlinear state model

$$\left.\begin{array}{rcl} \dot{V} &=& \frac{\bar{q}S\bar{c}q}{2mV}\left[C_{xq}(\alpha)\cos\alpha + C_{zq}(\alpha)\sin\alpha\right] \\ &+& \frac{\bar{q}S}{m}\left[C_x(\alpha,\delta_e)\cos\alpha + C_z(\alpha,\delta_e)\sin\alpha\right] \\ &-& g\sin(\theta-\alpha) + \frac{T}{m}\cos(\alpha) \\ \dot{\alpha} &=& q\left[1 + \frac{\bar{q}S\bar{c}}{2mV^2}\left(C_{zq}(\alpha)\cos\alpha - C_{xq}\sin\alpha\right)\right] \\ &+& \frac{\bar{q}S}{mV}\left[C_z(\alpha,\delta_e)\cos\alpha - C_x(\alpha,\delta_e)\sin\alpha\right] \\ &+& \frac{g}{V}\cos(\theta-\alpha) - \frac{T}{mV}\sin(\alpha) \\ \dot{\theta} &=& q \\ \dot{q} &=& \frac{\bar{q}S\bar{c}q}{2I_yV}\left[\bar{c}C_{mq}(\alpha) + \Delta C_{zq}(\alpha)\right] \\ &+& \frac{\bar{q}S\bar{c}}{I_y}\left[C_m(\alpha,\delta_e) + \frac{\Delta}{\bar{c}}C_z(\alpha,\delta_e)\right] \\ \dot{h} &=& V\sin(\theta-\alpha) \end{array}\right\} \quad (1)$$

where V, α, θ, q and h are the aircraft's velocity, angle-of-attack, pitch attitude, pitch rate and altitude respectively, T the thrust force, δ_e the elevator angle, m the mass of the aircraft, I_y the moment of intertia about the Y-body axis, $\bar{q} = \bar{q}(h,V) = \frac{1}{2}\rho(h)V^2$ the dynamic pressure, S the wing area, Δ the distance between the reference and actual center of gravity, $C_m(\cdot)$ the pitching moment coefficient along the Y-body axis, $C_{mq}(\cdot) = \frac{\partial C_m}{\partial q}$ the variation of C_m with pitch rate, $C_x(\cdot)$ and $C_z(\cdot)$ the force coefficients along the stability X and Z axes respectively, and $C_{xq}(\cdot)$ and $C_{zq}(\cdot)$ the variations of these coefficients with the pitch rate. Defining the state x, input u and output y [1] respectively as

$$x = [V\ \alpha\ \theta\ q\ h]^T \in R^5,\ u = [T\ \delta_e]^T \in R^2,\ y = [V\ h]^T \in R^2$$

the system (1) can be compactly written in standard form as

$$\dot{x} = f(x,u),\ y = h(x,u) \quad (2)$$

For the purpose of simulating our controller design, we build a Simulink model for the longitudinal dynamics of a scaled F-16 aircraft model based on the NASA Langley wind tunnel tests in [16], and described in [20], [29]. Our model differs from the ones in [20], [29] primarily in that

1) We only build a 3-DOF 5th order longitudinal model (so $\beta = 0$) as opposed to the 6-DOF model for the full 12th order nonlinear state model.
2) We do not include actuator models, in particular, we ignore lag effects and rate saturation (we include magnitude saturation though). For example, the NASA data [16] includes a model of the F-16 afterburning turbofan engine, in which the thrust response is modeled as a first-order lag, and the lag time constant is a function of the actual engine power level, and the commanded power. The command power is related to the throttle position δ_{th}, which is taken as the input in place of the thrust T, and the inclusion of the engine model increases the system order by one. As will be evident from the control design in Section 3, the inclusion of actuator dynamics (usually modled as first-order lag filters) can easily be incorporated in our design. We do not do so since it detracts from our intended contribution, which is the use of the conditional integrator apporach to improve transient performance.
3) We ignore the leading flap edge deflection. The F-16 has a leading-edge flap that is automatically controlled as a function of α and Mach and responds rapidly to α changes during maneuvering (see [20], [27] for a further discussion), and
4) We consider a smaller dynamic range for the angle of attack, $\alpha \in [-10^\circ, 45^\circ]$.

In particular, the model that we build corresponds to the *low fidelity* F-16 longitudinal model in [20], and to the longitudinal F-16 model developed in [13], but without thrust vectoring. For the aerodynamic data we use the approximate data in [16], [29], with the mass and geometric properties as listed in Table I.

TABLE I
Mass and Geometric Properties.

Parameter	Symbol	Value
Weight	W (lb)	20500
Moment of inertia	I_y (slug-ft^2)	55814
Wing area	S (ft^2)	300
Mean aerodynamic chord	$\bar{c}$ (ft)	11.32
Reference CG location	$x_{cg,ref}$	$0.35\bar{c}$

The coefficients $C_{xq}(\alpha)$, $C_{zq}(\alpha)$, $C_{mq}(\alpha)$, $C_x(\alpha,\delta_e)$, $C_z(\alpha,\delta_e)$, and $C_m(\alpha,\delta_e)$ are taken from [16], [29], and are included in [17, Appendix A.1] in tabular form. In the simulation, the data is interpolated linearly between the points, and extrapolated beyond the table boundaries.

Control design for (1) is challenging because the system is nonlinear, and moreover, non-affine in the input. While we believe that a controller design based on an affine approximation of the form $\dot{x} = f_0(x) + g_0(x)(u + g_\delta(x,u))$ is feasible [2], we do not pursue that here, and instead adopt the more common linearization based approach. In order to perform the linearization, we make the following assumption.

Assumption 1: Given any desired equilibrium value $\hat{y} = [\hat{V}, \hat{h}]^T$, there exist a unique equilibrium input $u = \hat{u}$ and state $x = \hat{x}$, such that $f(\hat{x},\hat{u}) = 0$, and $\hat{y} = h(\hat{x},\hat{u}) = 0$.

Defining the perturbation input, state, and output respectively by

$$u_\delta = u - \hat{u},\ x_\delta = x - \hat{x},\ y_\delta = y - \hat{y} \quad (3)$$

and expanding (2) in a Taylor series about $(\hat{x},\hat{u})$, and neglecting the higher order terms yields the linear approximation

$$\dot{x_\delta} = Ax_\delta + Bu_\delta,\ y_\delta = Cx_\delta + Du_\delta \quad (4)$$

[1] We use h and V as the "linearizing outputs", but the "regulated outputs" are the pitch-rate q and the velocity V.

[2] A design for non-affine systems that partially uses the idea above can be found in [31].

where

$$A = \frac{\partial f}{\partial x}(\hat{x},\hat{u}),\ B = \frac{\partial f}{\partial u}(\hat{x},\hat{u}),\ C = \frac{\partial h}{\partial x}(\hat{x},\hat{u}),\ D = \frac{\partial h}{\partial u}(\hat{x},\hat{u}) \tag{5}$$

Since the drag coefficients $C_i(\cdot)$ are not specified explicitly as functions of their arguments, but in tabular form (as look-up data), we use numerical techniques to solve for the trim (equilibrium) points and to compute the linearization. The *flight envelope* that we use for computing the trim conditions and the linearization is the cross product set $(\hat{V},\hat{h}) \in \Omega_V \times \Omega_h$, where $\Omega_V = [300, 900]$ ft/s in steps of 100, while $\Omega_h = [5000, 40000]$ ft in steps of 5000.

It is well-known that it is possible to do a *modal decomposition* of the linearized multi-input, multi-output (MIMO) flight dynamics into its component "short-period" and "phugoid" modes, which (i) reduces the MIMO system into two (essentially) single-input, single-output (SISO) systems, but more importantly (ii) offers physical insight into the dynamic behavior of the aircraft. In particular, it can be verified [3] that the MIMO linearization can be decoupled into the SISO-like state equations

$$\begin{aligned} \dot{z}_{1\delta} &= \begin{bmatrix}\dot{\alpha}_\delta \\ \dot{q}_\delta\end{bmatrix} \approx A_{11}\begin{bmatrix}\alpha_\delta \\ q_\delta\end{bmatrix} + B_{12}\ \delta_{e_\delta} \\ \dot{z_{2\delta}} &= \begin{bmatrix}\dot{V}_\delta \\ \dot{\theta}_\delta\end{bmatrix} \approx A_{21}\begin{bmatrix}\alpha_\delta \\ q_\delta\end{bmatrix} + A_{22}\begin{bmatrix}V_\delta \\ \theta_\delta\end{bmatrix} + B_{21}\ T_\delta + B_{22}\ \delta_{e_\delta} \end{aligned} \tag{6}$$

with the dynamics of the variables z_1 and z_2 constituting the short-period and phugoid modes respectively. Note that we did not include the altitude equation in (6). This is because (i) h is not a regulated output, and (ii) from (6), h does not enter the short-period and phugoid approximations explicitly, and is therefore not important for the control design.

We exploit the decoupling in (6) in our controller designs in the next section. In particular, we use the elevator δ_e to control the pitch rate q, and the thrust T to control the aircraft's velocity V. We emphasize that this decoupling, along with knowledge about the relative degree and high-frequency gain of the short-period dynamics, are the only aspects of the linearization that are used in our SMC design in the next section. The linearization is also explicitly used to design a classical gain-scheduled controller against which we compare our SMC design. Our design, while based implicitly on (6), is evaluated on the full fifth order nonlinear state model (2).

III. Control Design

Our primary control objective in this work is the design of a pitch-rate command system. It is well-known that a deadbeat response to pitch-rate commands is well suited to precise tracking of a target by means of a sighting device, and that control of the pitch rate is also the preferred system for approach and landing. Since the original system is MIMO, we also consider, but as a secondary objective, a Mach-hold autopilot, which is chiefly used on military aircraft during climb and descent. During a climb the throttles may be set at a fairly high power level, with the constant Mach number providing the best fuel efficiency. Similarly, a descent will be flown at constant Mach with the throttles near idle.

For the pitch-rate command system, the entire dynamic response is important, and we assume that the desired specifications are encapsulated in a reference model. We employ the same reference model as in [3]

$$G_m(s) = \frac{q_m(s)}{q_d(s)} = \frac{1.4s+1}{s^2+1.5s+1}$$

where q_d is the pitch rate pilot command. Our approach to control design for the pitch-rate is based on minimum-phase systems transformable to the normal form

$$\begin{aligned} \dot{\eta} &= \phi(\eta,\xi) \\ \dot{\xi} &= A_c\xi + B_c\ \gamma(x)\ [u-\alpha(x)] \\ y &= C_c\xi \end{aligned}$$

where $x \in R^n$ is the state, u the input, ρ is the system's relative degree, $\xi \in R^\rho$ the output and its derivatives up to order $\rho-1$, $\eta \in R^{n-\rho}$ the part of the state corresponding to the internal dynamics, and the triple (A_c, B_c, C_c) a canonical form representation of a chain of ρ integrators. A SMC design for such systems was carried out in [22], with the assumption that the internal dynamics $\dot{\eta} = \phi(\eta,\xi)$ are input-to-state stable (ISS) with ξ as the driving input. We apply this design to the short period approximation (6), with δ_{e_δ} as input and q_δ as output. Note that this is a relative degree $\rho = 1$ system. In order to apply the technique in [22], we need to transform the system to normal form and check internal stability. The next assumption states these properties.

Assumption 2: Consider the short-period approximation

$$\begin{bmatrix}\dot{\alpha}_\delta \\ \dot{q}_\delta\end{bmatrix} \stackrel{\text{def}}{=} \begin{bmatrix}a_{\alpha\alpha} & a_{\alpha q} \\ a_{q\alpha} & a_{qq}\end{bmatrix}\begin{bmatrix}\alpha_\delta \\ q_\delta\end{bmatrix} + \begin{bmatrix}b_{\alpha\delta} \\ b_{q\delta}\end{bmatrix}\delta_{e_\delta}$$

with output q_δ. Then (i) $b_{q\delta} < 0$, (ii) the (invertible) change of coordinates

$$\begin{bmatrix}\xi \\ \eta\end{bmatrix} \stackrel{\text{def}}{=} \begin{bmatrix}0 & 1 \\ 1 & -\frac{b_{\alpha\delta}}{b_{q\delta}}\end{bmatrix}\begin{bmatrix}\alpha_\delta \\ q_\delta\end{bmatrix}$$

transforms the system to normal form

$$\begin{aligned} \begin{bmatrix}\dot{\eta} \\ \dot{\xi}\end{bmatrix} &\stackrel{\text{def}}{=} \begin{bmatrix}a_{\eta\eta} & a_{\eta\xi} \\ a_{\xi\eta} & a_{\xi\xi}\end{bmatrix}\begin{bmatrix}\eta \\ \xi\end{bmatrix} + \begin{bmatrix}0 \\ 1\end{bmatrix}\delta_{e_\delta} \\ q_\delta &= \xi \end{aligned}$$

and (iii) $a_{\eta\eta} < 0$, i.e., the system is minimum-phase.

As before, we have verified parts (i) and (iii) of Assumption (2) numerically, for each trim condition, but an analytic discussion based on the stability derivatives can be found in [29].

Assumption (2) allows us to use the SMC controller design in [22] for the q-dynamics. For completeness, we briefly point out the ingredients of this design. In the absence of integral control, a standard SMC design for such a system takes the form

$$u = k\ \text{sgn}(s),\ \ s = e$$

[3] While an analytical discussion can be found in any standard textbook, such as [29, Chapter 4], this approximate decoupling been verified numerically in [17] for the F-16 model (1), for each operating condition.

where $e = q - q_m$ is the tracking error [4], and $\mathrm{sgn}(s)$ the signum function. It is easy to show that the design achieves asymptotic error regulation for "sufficiently large" k. In order to alleviate the chattering problem (see [32]) that is common with ideal discontinuous control, it is common to replace the above design with its continuous approximation

$$u = k \ \mathrm{sat}\left(\frac{s}{\mu}\right)$$

where $\mathrm{sat}(s)$ is the standard saturation function, and μ the width of the "boundary layer". This modification can reduce chattering, but at the expense of only achieving practical regulation of the error e, with $|e| = O(\mu)$. Consequently, reducing the steady-state error requires making μ small, which again leads to chattering. In order to achieve asymptotic error regulation with continuous SMC, robustly in the presence of disturbances and unknown parameter values, one can augment the system with an integrator driven by the error, i.e. $\dot{\sigma} = e$, and include the integrator output σ as part of the sliding variable s. Such a design can be found in [10], where it is shown that the design reduces to a saturated high-gain PI controller. The drawback of this design is that the recovery of the steady-state asymptotic error regulation (of ideal SMC) is achieved at the expense of transient performance degradation, in part due to an increase in system order, and in part as a consequence of controller saturation interacting with the integrator, resulting in "integrator windup".

The "conditional integrator" design in [22] is a novel way to introduce integral action in continuous SMC, while retaining the transient response of ideal SMC (without integral control). In this approach, we modify the sliding surface design to

$$s = k_0\sigma + e \tag{7}$$

where $k_0 > 0$ is arbitrary, and σ is the output of

$$\dot{\sigma} = -k_0\sigma + \mu\mathrm{sat}(s/\mu), \ \sigma(0) = 0 \tag{8}$$

To see the relation of (8) to integral control, observe that inside the boundary layer $\{|s| \leq \mu\}$, (8) reduces to $\dot{\sigma} = e$, which implies that $e = 0$ at equilibrium. Thus (8) represents a "conditional integrator" that provides integral action only inside the boundary layer. The control is simply taken as the continuous approximation of ideal SMC, i.e.,

$$\delta_e = k\mathrm{sat}(s/\mu) = k\mathrm{sat}\left(\frac{k_0\sigma + e}{\mu}\right) \tag{9}$$

This completes the design of the pitch-rate controller. With this design, we don't need to make μ small to achieve zero steady-state error, only "small enough" to stabilize the equilibrium point. The effect of this observation on robustness to switching imperfections such as time delays will be demonstrated through simulation in Section 4.

While analytical results for stability and performance of the above SMC design are given in [22, Theorems 1, 2], they are not directly applicable to the work in this paper since they were done for control affine systems. Consequently, we use the (control affine) linear approximation (6) as the starting point of our design, and verify the efficacy of the design through simulations. A mention of stability and boundedness under this design is made in the concluding paragraph of this section.

Since we are only interested in the Mach-hold autopilot (for V) as a secondary objective (of minor importance), and this is usually designed simply to meet specifications on steady-state error and disturbance rejection, we only design a simple PI controller for the thrust T to regulate V. However, extending this to a "better" controller design is straightforward.

It is easy to check that the equation for V_δ in (6) is of the form

$$\dot{V}_\delta \stackrel{\mathrm{def}}{=} a_{V\alpha}\alpha_\delta + a_{Vq}q_\delta + a_{VV}V_\delta + a_{V\theta}\theta_\delta + b_{VT}T_\delta + b_{V\delta}\delta_{e_\delta} \tag{10}$$

and it can be verified that for each trim condition, $a_{VV} < 0$, i.e., the V_δ-subsystem is stable. We view the term $a_{V\alpha}\alpha_\delta + a_{Vq}q_\delta + a_{V\theta}\theta_\delta + b_{V\delta}\delta_{e_\delta}$ as constituting a "matched disturbance", and simply augment the stability of this system by designing T_δ as the PI controller

$$T_\delta = -k_P V_\delta - k_I\sigma_V, \ \dot{\sigma}_V = V_\delta \tag{11}$$

with the gains $k_p, k_I > 0$ chosen to assign the eigenvalues of the 2nd-order system with states σ_V and V_δ at desired pole locations. The control is then taken as $T = \hat{T} + T_\delta$. Clearly, an alternate implementation where we don't need the nominal control $\hat{T} = \hat{T}(\hat{h}, \hat{V})$ is to simply use the control

$$T = -k_P V_\delta - k_I\sigma_V, \ \dot{\sigma}_V = V_\delta$$

Since we don't wish to gain-schedule, we use the alternate implementation, with the control saturated at its physically allowable limits. This completes the design of the Mach-hold autopilot controller.

As previously mentioned, the analytical results of [22] do not directly apply to this design. However, assuming that the short-period and phugoid decomposition approximately holds, a naive argument that our controller design achieves boundedness of all states, and asymptotic error regulation of the error e is presented below. The SMC (9) achieves robust regulation of the pitch-rate q, provided the value of k is "sufficiently large" [5]. The variable α is bounded since the system is minimum-phase. The variable θ evolves according to $\dot{\theta} = q$, and hence is bounded whenever q is. The PI controller (11) achieves boundedness of the velocity V. Finally, from the equation of $\dot{h}$, it follows that h is bounded for all finite time whenever V is, so that with our SMC and PI controllers for δ_e and T respectively, all the states of the closed-loop system are bounded. Our simulation results, which we present next, appear to validate the above conclusions.

IV. Simulation Results

We present simulation results showing the effectiveness of our SMC design. Our design is compared against a more classical gain-scheduled approach to model following, with the details of the design described in [17, Chapter 3]. Briefly, this

[4] Note that for each trim condition $\hat{q} = 0$, so that $q_\delta \equiv q$, which is why we simply use q in defining e.

[5] Alternately, when the gain k is fixed apriori, one can estimate the corresponding region of attraction, see [22].

is a 2-DOF linear controller of the form $Ru_\delta = Tu_{\delta m} - Sy_\delta$, where $u_{\delta m}$ is the command input, and R, S, and T are polynomials chosen such that the closed-loop transfer function (at each trim-condition) equals that of the reference model. In order to ensure performance robustness, the controller contains an integrator, i.e., $R = s\bar{R}$ for some $\bar{R}$. The controller coefficients are automatically computed for each trim condition by a matlab program, and continuously scheduled using a 2-dimensional linear interpolation with (h, V) as the scheduling variables.

Numerical values of the SMC parameters that we use in all the simulations are $k_0 = 10$, and that $k = 25$, so that $-25 \leq \delta_e \leq 25$, which are the limits mentioned in [20], [27]. The thrust T is assumed to be constrained as $T \in [0,\ 1000]$ lbs. The boundary layer width μ is chosen "sufficiently small", and we will say more on this shortly. The initial values in all simulations correspond to trim conditions with $(\hat{V}, \hat{h}) = (600ft/s, 20000ft)$. For ease of presentation, we first present our results with just the continuous SMC with no integral action, so that $u = -k\ \text{sat}\left(\frac{e_1}{\mu}\right)$, and then repeat the simulations with the conditional integrator design (9).

A. SMC Without Integral Control

Case 1: Short-period approximation with plant uncertainties: Our first simulation compares the SMC design with the polynomial-based approach when implemented on the 2nd-order linear SISO short-period approximation (6) of q with δ_e as the control input, when there are uncertainties in the aircraft model. For example, it is well-known (see, for example [7]) that the pitching moment C_m is associated with as much as 70% and 80% uncertainty on its lower and upper bounds respectively, i.e.,

$$0.3C_m \stackrel{\text{def}}{=} \underline{C}_m \leq C_m \leq 1.8C_m \stackrel{\text{def}}{=} \overline{C}_m$$

where C_m is the nominal value used in the look-up table. Such uncertainties will lead to errors in both the linearization, and the trim values of the inputs, and hence a loss of nominal performance. For the purpose of simulation, we simply model the uncertainties as random perturbations of the coefficients of A_{11} in (6) to within 50% of their nominal values. The pilot pitch-rate command q_d is a doublet of magnitude 30 deg/s. Figure 1 shows the tracking errors for the values $\mu = 0.1$ and $\mu = 0.01$. It is clear that (i) the SMC has **much better transient performance** compared to the polynomial approach (we have clipped the y-axis limits at ± 1, otherwise the plots for the two values of μ are indistinguishable), and (ii) as we decrease μ, the performance of the SMC gets better (with $\mu = 0.01$, the error is almost identically zero !). However, recall that too small a value of μ could result in chattering, when there are switching imperfections such as delays, something that we will show by simulation shortly. Note that the SMC design does not use any information about the linearization except for the relative degree and the sign of the high-frequency gain $b_{q\delta}$.

Case 2: Full linear model with input-additive disturbance: In order to demonstrate the performance of the robustness of the SMC approach to matched disturbances, we assume

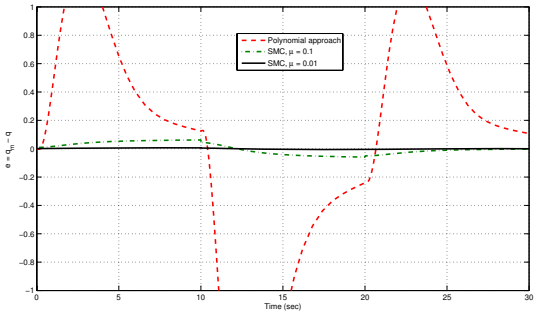

Fig. 1. Short-period approximation with uncertainties.

that there is an input additive disturbance at the elevator input (which can alternately be thought of as offset of the trim value of δ_e), i.e., $\delta_e = \hat{\delta}_e + d$. The SMC and polynomial designs are now tested on the (full) 5th-order MIMO linearized model (4)-(5) instead of just the short-period approximation (6). Figure 2 shows the simulation results for $d = 5$, and it is again clear that the SMC far outperforms the polynomial approach based controller design.

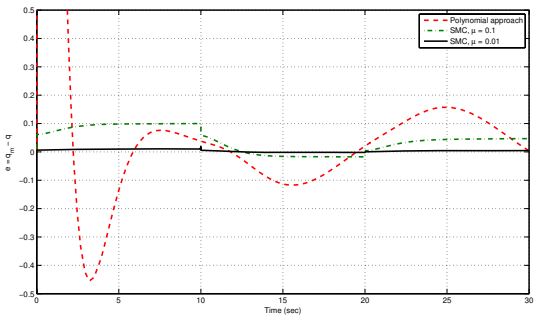

Fig. 2. Full linear model with input additive disturbance.

Case 3: Full Nonlinear Model: Next, we demonstrate the performance of our controller on the full nonlinear model (1). Figure 3 shows the simulation results for 2 different values of magnitude of q_d, 5 deg/s and 30 deg/s, and 2 different values of μ in the SMC design, and we see that the performance of the SMC is superior to the polynomial approach. As before, we have had to clip the y-axis limits in the error subplots so that the difference between the errors for $\mu = 0.1$ and $\mu = 0.01$ can be observed. For the first error subplot, corresponding to $q_d = 5$, the error for the polynomial approach is roughly between $\approx \pm 1$, while we have limited the plot axis to ± 0.1. Similarly, for the error subplot corresponding to $q_d = 30$, the error for the polynomial approach is roughly between $\approx \pm 7$, while we have limited the plot axis to ± 0.7. By contrast, the error for the SMC with $\mu = 0.1$ is roughly less than 0.02 for $q_d = 5$, and less than 0.1 for $q_d = 30$ in "steady-state". By steady-state, we refer to the period $t > 2$s. The reason for the relatively large error of about 0.5 (which itself is roughly 14 times smaller than the error with the polynomial approach !) is that the control reaches its saturation limits (in particular,

$\delta = -25^\circ$ between 0.7 and 1.35s) with the SMC approach. We do not apply saturation limits for the polynomial approach. In other words, this simulation shows that SMC with no gain-scheduling, and with imposed saturation limits, outperforms the gain-scheduled polynomial approach controller without saturation.

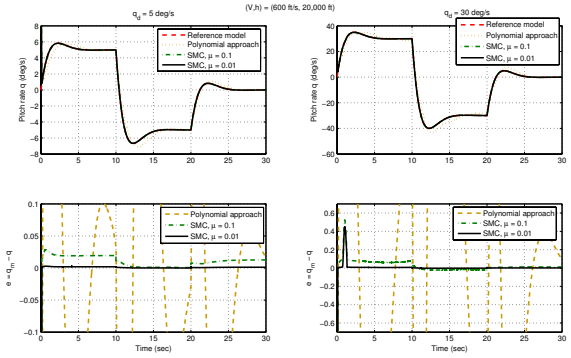

Fig. 3. Nonlinear model: $q_d = 5$, and $q_d = 30$ deg/s.

B. SMC With Conditional Integrator

1: Full Nonlinear Model: We repeat the last simulation of the preceding subsection (performance with the nonlinear model), but with the conditional integrator. Since we have already plotted the results of SMC without integral control and shown that they are superior to the polynomial approach, we simply compare the errors for the SMC with and without integral control, and only do so for $q_d = 30$ deg/s. The simulation results are done for $\mu = 1$ and $\mu = 0.1$. The reason to include a larger value of μ is twofold (i) to demonstrate the fact that the inclusion of integral action means that we don't need to make μ very small to achieve regulation, only small enough to stabilize the equilibrium point, and (ii) to highlight the issue of chattering with small μ, which we relegate to the next simulation. The simulation results are shown in Figure 4, from which two inferences might be drawn. The first is that, in the absence of integral control, since $|e| = O(\mu)$, we must decrease μ in order to achieve smaller steady-steady state errors, and this is clear from the two subplots. The second inference is that the inclusion of integral action decreases the steady-state error, and in fact, achieves asymptotic error regulation.

2: Robustness to Switching Implementations and Chattering: Next, we show decreasing μ, while reducing the steady-state error in an ideal scenario, can lead to chattering when there are switching imperfections such as delays. To demonstrate this, we repeat the previous simulation with a delay of 5ms (which is not really very large) preceding the input. The simulation results are shown in Figure 5, and we see considerable chattering in the control for $\mu = 0.1$, and we see that the control frequently hits the saturation limits. This chattering can cause actuator wear, degrade system performance, excite unmodeled high-frequency dynamics, and even result in instability. In order that chattering be avoided, we must make μ large, but doing so without integral control

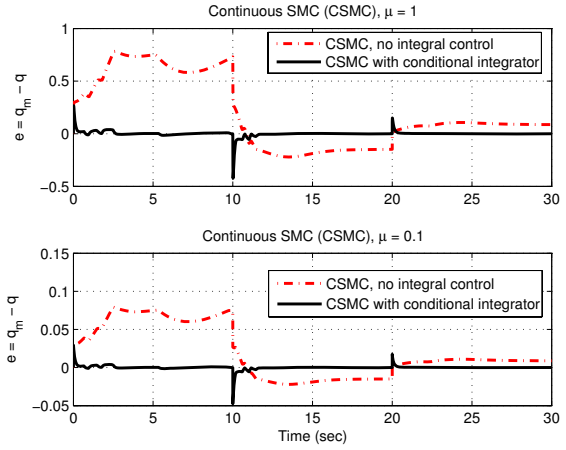

Fig. 4. Tracking errors with with conditional integrator SMC: Nonlinear model, $q_d = 30$ deg/s.

will lead to larger errors, since $|e| = O(\mu)$. The inclusion of integral control using conditional integrators offers a way to retain transient performance of ideal SMC and achieve zero steady-state error, without having to make μ very small, so that chattering can be avoided, and this is readily inferred from Figure 5.

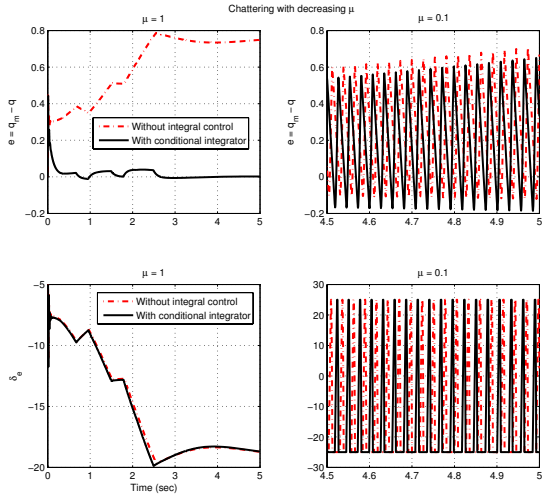

Fig. 5. Time-delays and chattering in continuous SMC.

3: Mach-hold Autopilot: Lastly, before we summarize our results, we present our results for velocity tracking with the PI controller, with gains $k_P = 828.4$ and $k_I = 191.2$ chosen to assign the roots of the closed-loop characteristic polynomial

$$\lambda^2 + b_{VT} k_P \lambda + b_{VT} k_I$$

at -0.3 and -1. The desired velocity reference is the output of the first order filter $H(s) = \frac{1}{s+1}$, to which the input is a doublet-like signal with an initial value of 600 ft/s, changing to 500 ft/s at $t = 17s$, and to 700 ft/s at $t = 35s$. The results are shown in Figure 6, and it is clear that this simple controller achieve robust regulation, even though its transient

performance is not very good, as expected. We can improve the design of the velocity controller using techniques like SMC or other robust linear techniques, but do not pursue it here, since velocity control is only a secondary objective.

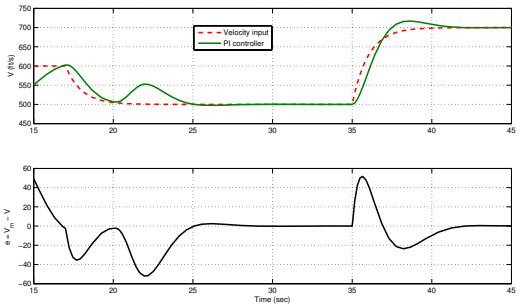

Fig. 6. Velocity (Mach-hold) autopilot response to velocity command: PI controller.

V. Conclusions

This paper presented a new SMC design for control of the pitch-rate of an F-16 aircraft, based on the conditional integrator design of [22]. The design exploits the short-period approximation of the linearized flight dynamics. The control has a very simple structure: it is simply a saturated high-gain PI controller with an anti-windup integrator; and the only precise information that it uses are the relative degree and sign of the high-frequency gain of the linearized short-period approximation. The robustness of the method to modeling uncertainty, disturbances, and time-delays was demonstrated through extensive simulation, and the simulation results showed that the method outperforms, without any scheduling requirement, the transient and steady-state performance of a conventional gain-scheduled model-following controller. The conditional integrator design allows us to introduce integral action to achieve zero steady-state errors without degrading the transient performance of ideal SMC. Consequently, we believe that the results presented in this paper are a promising start to demonstrate the efficacy of the conditional integrator based SMC design to flight control. In fact, while we presented our design for control of the pitch-rate, an extension of our results to regulation of the angle of attack can be found in [23], while an extension to control of the lateral flight dynamics can be found in [30].

References

[1] R.J. Adams, J.M. Buffington, and S.S Banda. Design of nonlinear control laws for high-angle-of-attack flight. *Jnl. Guidance, Control, and Dynamics*, 17(4):737–745, 1994.

[2] G.J. Balas. Flight control law design: An industry perspective. *European Jnl. of Ctrl.*, 9(2-3):207–226, 2003.

[3] C. Barbu, S. Galeani, A.R. Teel, and L. Zaccarian. Non-linear anti-windup for manual flight control. *Intl. Jnl. of Ctrl.*, 78(14):1111–1129, 2005.

[4] R. Bhattacharya, Balas. G., M. Kaya, and A. Packard. Nonlinear receding horizon control of an F-16 aircraft. *Jnl. Guidance, Control, and Dynamics*, 25(5):924–931, 2002.

[5] J.M. Biannic and P. Apkarian. Parameter varying control of a high performance aircraft. In *Proc. AIAA, Guidance, Navigation and Control Conference*, pages 69–87, 1996.

[6] Y.J. Huang, T.C. Kuo, and H.K. Way. Robust vertical takeoff and landing aircraft control via integral sliding mode. *Control Theory and Applications, IEE Proceedings-*, 150:383–388, 2003.

[7] Y. Huo, M. Mirmirani, P. Ioannou, and R. Colgren. Adaptive linear quadratic design with application to F-16 fighter aircraft. In *AIAA Guidance, Navigation, and Control Conference and Exhibit*, August 2004.

[8] E.M. Jafarov and R. Tasaltin. Robust sliding-mode control for the uncertain MIMO aircraft model F-18. *IEEE Trans. Aerospace Electronic Sys.*, 36(4):1127–1141, 2000.

[9] T. Keviczky and G. Balas. Receding horizon control of an F-16 aircraft: A comparative study. *Control Engg. Practice*, 14(9):1023–1034, 2006.

[10] H.K. Khalil. Universal integral controllers for minimum phase nonlinear systems. *IEEE Trans. Aut. Ctrl.*, 45(3):490–494, 2000.

[11] D.A. Lawrence and W.J. Rugh. Gain scheduling dynamic linear controllers for a nonlinear plant. *Automatica*, 31(3):381–390, 1995.

[12] T. Lee and Y. Kim. Nonlinear adaptive flight control using backstepping and neural networks controller. *Jnl. Guidance, Control, and Dynamics*, 24(4):675–682, 2001.

[13] B. Lu. *Linear Parameter-Varying Control of an F-16 Aircraft at High Angle of Attack*. PhD thesis, North Carolina State University, 2004.

[14] B. Lu, F. Wu, and S. Kim. LPV antiwindup compensation for enhanced flight control performance. *Jnl. Guidance, Control and Dynamics*, 28:495–505, 2005.

[15] J-F. Magni, S. Bennani, and J. Terlouw (Eds). *Robust Flight Control: A Design Challenge*. Lecture Notes in Control and Information Sciences - Vol 224. Springer, 1998.

[16] L.T. Nguyen, M.E. Ogburn, W.P. Gillert, K.S. Kibler, P.W. Brown, and P.L. Deal. Simulator study of stall/post-stall characteristics of a fighter airplane with relaxed longitudinal static stability. *NASA Technical Paper 1538*, 1979.

[17] E. Promtun. *Sliding Mode Control of F-16 Longitudinal Dynamics*. MS. Thesis, San Diego State University, San Diego, USA, 2007.

[18] E. Promtun and S. Seshagiri. Sliding mode control of pitch-rate of an F-16 aircraft. In *17th IFAC World Congress*, Seoul, S. Korea, July 2008.

[19] W.C. Reigelsperger and S.S. Banda. Nonlinear simulation of a modified F-16 with full-envelope control laws. *Control Engineering Practice*, 6:309–320, 1998.

[20] Richard S. Russell. Non-linear F-16 simulation using Simulink and Matlab. Technical report, University of Minnesota, June 2003.

[21] R. Rysdyk and A.J. Calise. Robust nonlinear adaptive flight control for consistent handling qualities. *IEEE Trans. Aut. Ctrl.*, 13(6):896–910, 2005.

[22] S. Seshagiri and H.K. Khalil. Robust output feedback regulation of minimum-phase nonlinear systems using conditional integrators. *Automatica*, 41(1):43–54, 2005.

[23] S. Seshagiri and E. Promtun. Sliding mode control of F-16 longitudinal dynamics. In *2008 American Control Conference*, Seattle, Washington, U.S.A, June 2008.

[24] J.S. Shamma and J.S. Cloutier. Gain-scheduled bank-to-turn autopilot design using linear parameter varying transformations. *Jnl. Guidance Control and Dynamics*, 9(5):1056–1063, 1996.

[25] Y. Shtessel, J. Buffington, and S. Banda. Tailless aircraft flight control using multiple time scale reconfigurable sliding modes. *IEEE Trans. Ctrl. Sys. Tech.*, 10(2):288–62, 2002.

[26] S.A. Snell, D.F. Enns, and Jr. W.L. Garrard. Nonlinear inversion flight control for a supermaneuverable aircraft. *Jnl. Guidance, Control, and Dynamics*, 15(4):976–984, 1992.

[27] Lars Sonneveldt. Nonlinear F-16 model description. Technical report, Delft University of Technology, The Netherlands, June 2006.

[28] M.S. Spillman. Robust longitudinal flight control design using linear parameter-varying feedback. *Jnl. Guidance, Control, and Dynamics*, 23(1):101–108, 2000.

[29] B.L. Stevens and F.L. Lewis. *Aircraft Control and Simulation*. John Wiley & Sons, Inc., 2 edition, 2003.

[30] H. Vo and S. Seshagiri. Robust control of F-16 lateral dynamics (accepted). In *2008 IEEE IECON08*, Orlando, Florida, U.S.A, Nov 2008.

[31] A. Young, C. Cao, N. Hovakimyan, and E. Lavretsky. An adaptive approach to nonaffine control design for aircraft applications. In *AIAA Guidance, Navigation, and Control Conference and Exhibit*, Keystone, CO, USA, August 2006.

[32] K.D. Young, V.I. Utkin, and U. Ozguner. A control engineer's guide to sliding mode control. *IEEE Trans. Ctrl. Sys. Tech.*, 7(3):328–342, 1999.